On the Influence of the Sample Properties on the Measurement of the Implied Open-Circuit Voltage

Bernd Steinhauser, Armin Richter, Andreas Fell, and Martin Hermle

***Abstract*—The implied voltage iV_{OC} is a popular parameter for the electronic quality of solar cell test samples. It is used to characterize properties like the passivation quality of surface coatings. While iV_{OC} fundamentally depends on the sample properties besides the electronic quality of the interface, such influences have not been systematically quantified and are usually not stated, which questions the comparability of iV_{OC} across multiple sample sets. This article is dedicated to study the influence of the wafer doping and thickness, surface passivation and reflection as well as light trapping on iV_{OC} by device simulations using Quokka3, supported by experimental data. It is shown that, even moderate changes in these sample properties can result in a significant deviation in iV_{OC}. This is emphasized if multiple influences are combined, as shown on two samples featuring an iV_{OC} of 737 and 754 mV. This difference in iV_{OC} can be broken down into individual contributions, demonstrating how the aforementioned influences can quickly add up to 10–15 mV if combined. From this perspective, it is difficult to compare their respective surface passivation performance, which only accounts for less than 10% of the total change in iV_{OC}. Therefore, we recommend a precise description of the aforementioned sample properties when reporting iV_{OC} values in publication. To quantify the surface recombination, we recommend the use of J_{0s} instead of iV_{OC}, since it specifically describes surface recombination and is usually independent from the discussed sample properties.**

***Index Terms*—Circuit simulation, inductance measurements, silicon devices, voltage measurements.**

I. Introduction

THE implied open-circuit voltage iV_{OC} represents the quasi-fermi level splitting within a noncontacted semiconductor sample under illumination. It differs from the external open-circuit voltage V_{OC}, which is defined as the potential difference between two contacts of opposite polarity including potential drops at the contacts [1], [2]. Since the quasi-fermi level splitting cannot be measured directly it is commonly calculated from the excess charge carrier density Δn, which can be determined by contactless measurements using tools like the Sinton lifetime tester as demonstrated by Sinton and Cuevas [3] or by measuring the photoluminescence [4]. iV_{OC} is strongly influenced by charge carrier recombination just like the external open-circuit voltage V_{OC} and, thus is a figure of merit for the sample's recombination properties. In recent years, many silicon solar cell researchers started to use iV_{OC} in publications and presentations, mainly as a measure of the surface recombination rate and, thus the surface passivation quality, but also as a measure of the selectivity in case of passivating and selective contacts (when compared with the external V_{OC}) [1]. The main reason for these used cases is that it represents an easily accessible parameter closely related to the external V_{OC}, a device parameter determined as per standard for solar cells. Specifically for the use case of a measure of the surface passivation quality the accessibility plays an important role as other well-suited parameters like J_{0s} [5] require data modeling and thorough knowledge of the involved models [6]–[9].

To motivate the following investigations, the iV_{OC} of two samples is of interest. These samples correspond to very commonly used samples in the PV research community for the purpose of evaluating surface coatings: both being *n*-type, but one being a 4" float-zone (FZ) and the other one being an M2 Czochralski (Cz) wafer (details are discussed later on). The wafers were subjected to the TOPCon passivation process and then resulted in an iV_{OC} of 737 mV for the FZ wafer and 754 mV for the Cz wafer. So, this suggests that the Cz wafer features a substantially better passivation due to the higher iV_{OC}? Actually, in this case, this is a misleading conclusion. However, for a better understanding of the effects in place here, first an introduction to iV_{OC} is given. Then, the influences of individual sample properties are discussed: the base doping, wafer thickness, surface recombination, and surface reflectance, each of which is different for the two aforementioned samples. In addition, the influence of light trapping is discussed, which is relevant for thin wafers. These investigations allow us to better separate and appraise the combined influences and resolve where the difference in iV_{OC} originates from and how large the contribution of the surface recombination is.

II. Definition of the Implied Voltage

For semiconductors, assuming steady-state generation and uniform distribution of excess charge carriers, the quasi-Fermi levels for electrons in the conductance band E_{fc} and holes in the valence band E_{fv} can be used to define a potential difference

$$iV_{OC} = \frac{E_{fc} - E_{fv}}{q} \tag{1}$$

Manuscript received November 6, 2020; revised December 18, 2020; accepted January 16, 2021. Date of publication February 11, 2021; date of current version April 21, 2021. This work was supported by the German Federal Ministry for Economic Affairs and Energy under Contract 03EE1031A (PaSoDoble) and Contract 03EE1032 (CusTCO). *(Corresponding author: Bernd Steinhauser.)*

The authors are with the Fraunhofer-Institut für Solare Energiesysteme ISE, 79110 Freiburg, Germany (e-mail: bernd.steinhauser@ise.fraunhofer.de; armin.richter@ise.fraunhofer.de; andreas.fell@ise.fraunhofer.de; martin.hermle@ise.fraunhofer.de).

Color versions of one or more figures in this article are available at https://doi.org/10.1109/JPHOTOV.2021.3053094.

Digital Object Identifier 10.1109/JPHOTOV.2021.3053094

where q is the elementary charge. This potential difference iV_{OC} is usually called *implied open-circuit voltage*, as it is the open-circuit voltage that is *implied* by a certain splitting of the quasi-Fermi levels. If assuming Boltzmann statistics, iV_{OC} can be approximated as [3]

$$iV_{\mathrm{OC}}\ (\Delta n) = \frac{k_{\mathrm{B}}T}{q}\ \ln\left(\frac{n\cdot p}{n_{\mathrm{i,eff}}^2}\right) \cong \frac{k_{\mathrm{B}}T}{q}\ \ln\left(\frac{(N_{\mathrm{Dop}}+\Delta n)\cdot \Delta n}{n_{\mathrm{i,eff}}^2}\right) \quad (2)$$

where for the second part, it is assumed that the semiconductor is doped, meaning that either n or p dominates. Here, n and p are the electron and hole densities, Δn is the minority (or excess) charge carrier density, N_{Dop} is the wafer doping concentration, $n_{\mathrm{i,eff}}$ is the effective intrinsic charge carrier density, k_{B} is the Boltzmann constant, and T the temperature. Thus, for each Δn (and consequentially for each amount of excess generation) the relation defines an iV_{OC}. However, if a value for iV_{OC} is given, it usually refers to the iV_{OC} at 1 sun illumination. This is especially the case if the illumination or generation rate is not explicitly stated. The generation rate relates to the effective minority charge carrier lifetime τ_{eff} via the following:

$$G = R = \frac{\Delta n}{\tau_{\mathrm{eff}}}. \quad (3)$$

R and G denote the corresponding charge carrier recombination and generation rates and are equal since steady-state illumination was assumed. Thus, each pair of Δn and τ_{eff} is linked to a specific generation rate G and this means that the τ_{eff} defines which Δn (and, thus which iV_{OC}) corresponds to 1 sun illumination. Furthermore, the generation and recombination rate can be linked to the wafer thickness w and recombination parameter J_0 as follows:

$$G = R = \frac{\Delta n}{\tau_{\mathrm{eff}}}\, w = J_0\, \frac{n\cdot p}{n_{\mathrm{i,eff}}^2} \quad (4)$$

where R, τ_{eff}, and J_0 can be split up into individual contributions, e.g., surface (J_{0s}) and bulk (J_{0b0} , excluding the surface) recombination.

III. Experimental

Several TOPCon test samples for lifetime measurements were fabricated on FZ wafers. The general procedure for the fabrication of the samples is described in detail in [10] and will not be repeated here. The wafers were 100 mm in diameter and featured a shiny-etched surface without texturing and no additional optical layers unless specified explicitly. Other sample parameters such as wafer thickness, base resistivity, and doping type are varied within the experiments and are given with the respective datasets.

The minority charge carrier lifetime of the wafers was measured in the long-flash (applying generalized evaluation [11]) and short-flash (evaluation of the transient) mode of a WCT-120 Sinton lifetime tester. The optical factor for the generalized analysis was adjusted such that the two lifetime curves matched as well as possible. The measurements with the lifetime tester were done using a long-pass filter after the flash lamp as is standard for this setup to ensure homogeneous charge carrier generation. This spectrum is denoted as "QFlash/IR," whereas the spectrum without long-pass filter is denoted "QFlash/noIR" hereafter.

In case of samples featuring SiN_x single-sided, the samples were hydrogenated (as described in [10]) before the SiN_x deposition to fully activate the passivation on both sides. The SiN_x layer had a refractive index of approximately 2.0 and a thickness of 100 nm. The samples were then measured by QSSPC from both sides and the adjustment of the optical factor was done separately for each side, as different optical factors are required. To achieve comparable measurements, the samples were aligned to the center of the sample stage to ensure that the same sample area was measured for both sides. A sketch for the measurement setup is also given in Fig. 3. The reflectance of both the TOPCon side as well as the TOPCon/SiN_x side was measured using a PerkinElmer Lambda 950 UV–NIR spectrometer.

For the investigation of the combination of multiple effects, additional TOPCon lifetime samples were fabricated on Cz material with 156.75 × 156.75 mm^2 size and 150 μm final thickness. These wafers were saw-damage-etched in KOH prior to processing, the (FZ-specific) thermal pretreatment before passivation was omitted. These wafers were coated with SiN_x (n ≈ 2.0, 70 nm thickness) on both sides after the TOPCon passivation. Both the selected FZ sample and the selected Cz sample were measured by calibrated photoluminescence using the Fraunhofer ISE modulum [4]. To gather the iV_{OC} closely corresponding to the best-passivated surface, statistical methods were used, thus minimizing the influences of surface defects like scratches. For this, the statistic mode value, meaning the maximum of the iV_{OC} distribution and, thus the most probable value, was taken for each of the samples. If the number of defects is sufficiently low, this corresponds to the iV_{OC} the surface passivation can achieve. Since the FZ sample exceeded the bulk lifetime predicted by the Richter parameterization, J_{0s} extraction was not possible for this sample. Instead, the J_{0s} of 0.2 fA/cm^2 was extracted from a sister sample featuring the same surface morphology and surface passivation but lower doping and should thus be a good estimate of the J_{0s}. For the Cz sample, the lifetime curve was fitted using the approach by Kane and Swanson [8] and assuming the Auger and radiative parameterization of Richter [12] and Altermatt [13], respectively.

IV. Simulation Setup

To analyze the different influences, 1-D simulations were performed using Quokka 3 [14]. The simulated device is a silicon wafer at a temperature of 300 K with lumped skin layers defined on each side with the skin J_0 corresponding to $J_{0s} = 0.2$ fA/cm^2 if not specified otherwise. Intrinsic recombination was assumed for the bulk, incorporating the models by Richter [12] and Altermatt [13] for the Auger and radiative recombination, respectively. For the excitation, monochromatic illumination at a wavelength of 790 nm (as used by the modulum characterization tool) was assumed corresponding to 1 sun equivalent excitation unless

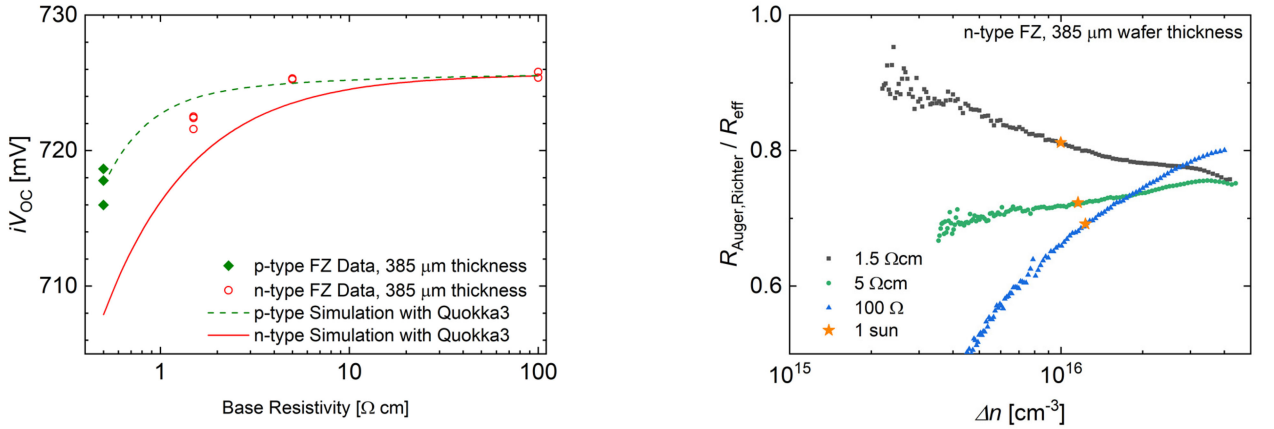

Fig. 1. Left: iV_{OC} determined by the Sinton lifetime tester on 385 μm thick FZ samples with varying doping type and doping concentration. For both 1.5 and 5 Ωcm, there are two overlapping data points each in the graph. The lines give the expected iV_{OC} simulated by Quokka3. Right: exemplary plot of the Auger recombination rate relative to the total/effective recombination rate for three of the measurements. The graph visualizes the amount of recombination due to Auger recombination (according to the Richter parameterization) at a certain Δn. The orange stars give the points corresponding to 1 sun illumination.

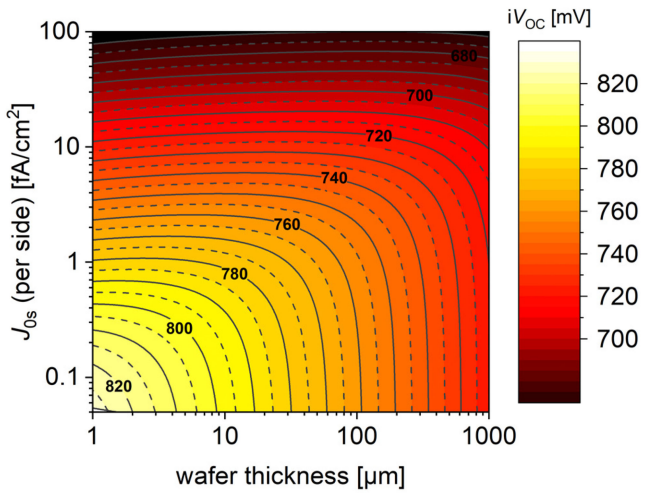

Fig. 2. Simulation of the iV_{OC} on 100 Ωcm n-type Si in dependence of the wafer thickness and J_0 assuming AM1.5g external illumination without any optical losses at the front and Lambertian light trapping according to Green [15] at the rear.

specified otherwise. The transmission on planar surface without optical layer was set to 67.7% unless specified otherwise. The value of 67.7% was determined by measuring the reflectance of a c-Si sample using a UV–NIR spectrometer as mentioned in the experimental section. For the light trapping, either Lambertian light trapping according to Green [15] or the parameterization by McIntosh (case 1: planar/planar surface with no reflector at the rear) [16] was assumed. Other sample parameters like the device thickness, base doping, and type were varied corresponding to the respective samples in discussion. For the thickness variation, photon recycling was investigated as a possibly relevant effect. This was implemented as an effective reduction in the radiative recombination rate (thus, a lower relative recombination factor B_{rel}) as this is expected to be equivalent to an effective increase in the generation rate due to the photon recycling under quasi-steady-state conditions. The used effective B_{rel} was derived by fitting an analytical optical model to spectral measurement of the reflectance and transmittance. Details on this procedure will be part of an upcoming publication.

V. Results and Discussion

A. Influence of the Base Doping

Figure 1(left) shows the iV_{OC} measured for a set of p- and n-type samples with base resistivity reaching from 0.5 Ωcm to 100 Ωcm. In both the experimental data and the simulation, a clear trend of increasing iV_{OC} with increasing base resistivity can be observed. For low base resistivities (< 10 Ωcm) on n-type silicon, there is a deviation between the simulation and the experimental data, where the simulation predicts lower iV_{OC} than what was measured. Figure 1(right) shows the measured lifetime curve relative to the Auger lifetime (i.e., $\tau_{\mathrm{eff}}/\tau_{\mathrm{Auger}}$) for one n-type sample of each base doping concentration. This corresponds to the quotient of the recombination rates $R_{\mathrm{Auger}}/R_{\mathrm{eff}}$ and indicates the percentage of the recombination the Auger recombination can be accounted for. The yellow stars mark the data points corresponding to 1 sun illumination. The curve for the highest doped sample shows the highest influence (0.8 to 0.9) of the Auger lifetime. Only at very high Δn of 2×10^{16} cm^{-3} or higher the influence of Auger for the lower doped samples increases to a similar range. The 1-sun points indicate the shift of Δn at 1 sun illumination due to the change in the base doping.

As there is a significant difference between simulation and experiment in Fig. 1, we want to discuss this first before discussing the actual influence. In Fig. 1(left), this difference is most prominent for n-type at higher base doping concentration. Photon recycling has to be considered as one effect, but this would only account for approximately 1–2 mV of the offset. As various groups have shown already, the predicted bulk lifetime by the Richter Auger model can be significantly exceeded [10], [17], [18]. Since this model is used in Quokka3, the simulation cannot

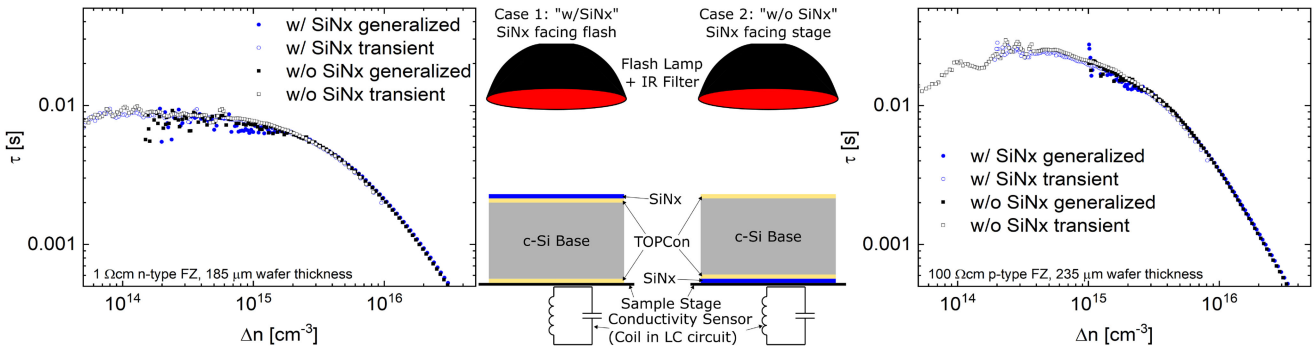

Fig. 3. Measurement of the effective minority charge carrier lifetime on 1 Ωcm *n*-type (left) and 100 Ωcm *p*-type (right) wafers that were symmetrically passivated by TOPCon and then single-sided coated by a typical SiN_x as used for antireflection coatings. Both samples were measured both in transient and generalized mode from both sides. A sketch is shown in the middle to illustrate these measurement setups. The optical factor was adjusted such that the corresponding transient and generalized curves match as well as possible.

fully reproduce the measured iV_{OC} due to an over-estimation of the Auger recombination rate at higher n-type base doping concentrations.

The second effect is present in Fig. 1(right). For the plotted ratio $R_{\mathrm{Auger}}/R_{\mathrm{eff}}$, it would be expected that with higher Δn all of the curves converge to 1, since the Auger recombination is expected to dominate at high Δn. However, it can be observed that instead the measured lifetime curve does not fully converge to the Auger lifetime in all of the cases, even after applying the correction for the distance sensitivity of the coil as proposed by Black et al. [19]. Since this offset was also observed for modulated photoluminescence (not shown here), this indicates a possible systematic deviation in the Auger model at this Δn range. Thus, with an updated Auger model, a better match of the simulation to the experimental data in Fig. 1(left) would be expected and the plots should converge to 1 for high Δn in Fig. 1(right).

As indicated in (2), there is a direct influence of the base doping on iV_{OC} and that a higher base doping should lead to a higher iV_{OC}. However, it has to be considered that an increase in the base doping can lead to an increase in the recombination rates as well. Here, three contributions have to be considered, surface recombination, Auger, and radiative recombination. The influence of the radiative recombination at 1 sun illumination can be neglected, whereas for the surface recombination, Macintosh showed that the influence of the base doping on the recombination parameter $J_{0\mathrm{s}}$ is negligible for typical surface passivation technologies and base doping concentrations [5]. This leaves the Auger recombination as a candidate and indeed an increase in the base doping leads to an increase in the Auger recombination rate [12]. This is also in-line with the trend observed in Fig. 1(right), which – despite the systematic deviations – clearly indicates that the Auger recombination is the dominating recombination mechanism at 1 sun. The stars also show the shift to a higher Δn at 1 sun illumination with decreasing base doping concentration. Whether this shift in Δn or the direct influence of the base doping on iV_{OC} dominates depends on the total recombination rate and, thus the level of Δn at 1 sun. In almost all cases, the shift in Δn leading towards a higher iV_{OC} with lower base doping [as observed in Fig. 1(left)] will be dominant. Only if the total recombination is very high (e.g., due to high surface or extrinsic bulk recombination) an increase in the base doping concentration can lead to an increase in iV_{OC}.

While the discussion so far focused solely on *n*-type material, Fig. 1(left) also indicates the influence for *p*-type material. Almost everything outlined in the previous paragraphs for *n*-type can be directly translated to *p*-type material. The exception is that for *p*-type, the Richter parameterization better describes the Auger recombination than for *n*-type, which is reflected in the simulated data better matching the experimentally determined values.

As a final remark, it should be noted that for the evaluated FZ samples extrinsic bulk recombination can be neglected. However, for solar grade silicon wafers, it might be necessary to consider this, even at 1 sun illumination. In such a case, the influence of the base doping concentration on iV_{OC} will depend on the specific defect and its concentration and, thus cannot be discussed here in detail.

B. *Influence of the Wafer Thickness and Surface Passivation*

The influence of the wafer thickness w on iV_{OC} and V_{OC} is possibly the best known influence of a sample parameter on $(i)V_{\mathrm{OC}}$. Experimental data are omitted here, as the topic was already thoroughly investigated by others, e.g., see [20]–[23]. Instead, simple simulation using Quokka3 were performed to illustrate and discuss the effect as well as that of the surface passivation. For the simulation, lowly doped *n*-type silicon ($\rho_{\mathrm{b}} = \ 100\ \Omega\mathrm{cm}$) without any extrinsic defect recombination and symmetrical passivation as described in the simulation setup was used.

The results for the simulation can be found in Fig. 2. The simulated data clearly show that both $J_{0\mathrm{s}}$ and w have a significant impact on iV_{OC} (and V_{OC}, if fabricating solar cells with the corresponding parameters). This influence is only small if either parameter is negligible (i.e., very small $J_{0\mathrm{s}}$ *or* very small w). Understanding the influence of $J_{0\mathrm{s}}$ is very straight forward as it is just a contribution to the total J_0, i.e., $J_0 = J_{0\mathrm{b}} = J_{0\mathrm{b0}} + 2 \cdot J_{0\mathrm{s}}$, where $J_{0\mathrm{b}}$ and $J_{0\mathrm{b0}}$ denote the recombination parameter for bulk contribution including and excluding the surface, respectively. The influence of w is indicated in (4). This

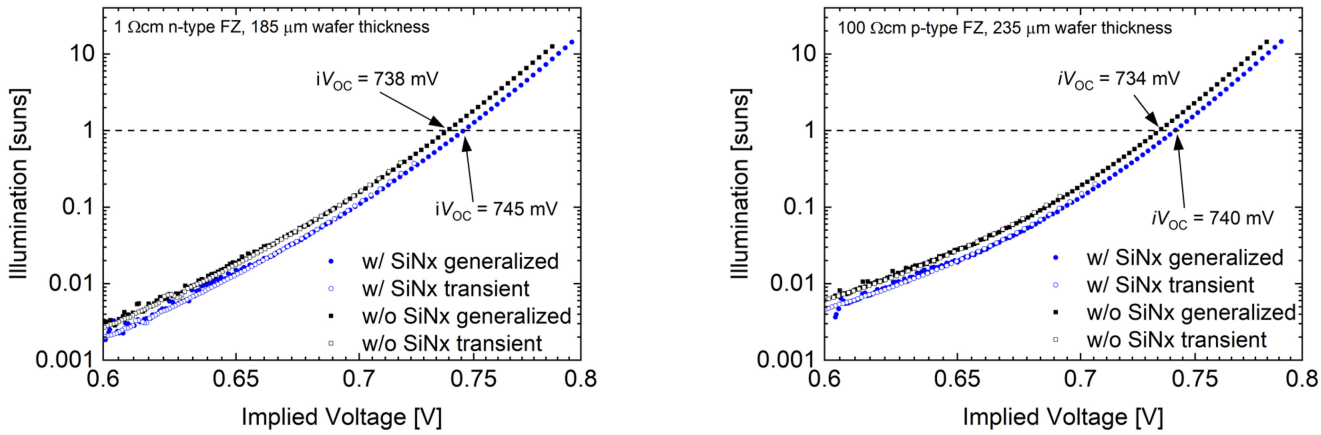

Fig. 4. The same data as shown in Fig. 3, but this time with the (external) generation plotted over the implied voltage, the well known "Suns-Voc" graph. 1 Ωcm *n*-type on the left, 100 Ωcm *p*-type on the right.

was analyzed in depth by Green [23], assuming high injection of the base, which is the case for our simulation.

The simulation in Fig. 2 shows that theoretically, it should be possible to reach an $iV_{\rm OC}$, even in the range of 800 mV, but this would require a very thin c-Si substrate with $w < 10$ μm, even if assuming ideal optics. The simulation also demonstrates that for typical wafer sizes of 150 to 200 μm almost no influence (indicated by the almost vertical contour lines) of $J_{0\rm s}$ is expected if $J_{0\rm s} < 1$ fA/cm^2, since $J_{0\rm b0}$ is dominating the recombination. This means that in this case $iV_{\rm OC}$ is not very sensitive to surface recombination and, thus is not a very good value to characterize it.

It should be mentioned that especially for a thickness variation as shown in Fig. 2, photon recycling (meaning reabsorption of photons generated by radiative recombination) has to be considered as a contribution to Δn. We investigated this and found that at 1 sun the effect is small (in the range of 1–2 mV) compared with the overall influence of the thickness on $iV_{\rm OC}$, since at this injection level Auger (and not radiative) recombination is the dominant intrinsic recombination path. However, for simulations and calculations of the implied fill factor and values at lower injection levels, it might be necessary to include photon recycling.

C. Influence of the Sample Optics

The next influence we want to investigate is that of the sample optics. For this, two samples were prepared that were symmetrically processed, apart from a SiN_x layer that was only deposited on one side of the wafer. The measured curves of the effective minority charge carrier lifetime for the two samples are shown in Fig. 3. The graphs show both the transient (open symbols, short flash) and the quasi-static (closed symbols, long flash, generalized evaluation) measurements from both the side with and without SiN_x. The match of the lifetime curves after adapting the optical factors is very good and the lifetime level is high, above 1 ms up to $\Delta n \approx 2 \times 10^{16}$ cm^{-3}.

Figure 4 shows the data from the same measurements, but this time, plotted as illumination intensity in suns vs. $iV_{\rm OC}$ in V. In contrast with the plot in Fig. 3, a significant shift between the curves measured from either side can now be observed. With SiN_x, the $iV_{\rm OC}$ for the 1 Ωcm *n*-type sample increased from 738 to 745 mV and for the 100 Ωcm *p*-type sample from 734 to 740 mV, i.e., a rather high difference of 6 to 7 mV. However, for further investigations of this effect, first it needs to be ensured that the measurements can be compared. When defining $iV_{\rm OC}$, one basic assumption was that of a uniform distribution of Δn. Since the samples are no longer symmetrical, it could be possible that one side exhibits more recombination than the other (e.g., due to more or less hydrogen available at the interface due to the SiN_x coating). As the Δn at 1 sun is relatively high, the lifetime is strongly limited by Auger recombination and, thus the effective minority charge carrier diffusion length $L_{\rm eff}$ could result in a significant nonuniformity of Δn, which would limit the comparability of the measurements. In case of the more critical measurement from the SiN_x side (due to the higher Δn at 1 sun), an $L_{\rm eff}$ of 1.2 mm can be calculated for the 1 Ωcm *n*-type wafer (w = 185 μm) as well as 2.2 mm for the 100 Ωcm *p*-type wafer (w = 235 μm). Thus, in both cases a uniform distribution of Δn over the wafer volume can be assumed. Differences in the recombination of the two sides should play a minor role, if present, especially since the Sinton lifetime tester uses a high-pass filter to ensure homogeneous generation of carriers. This is in-line with the observed match of the lifetime cures in Fig. 3.

Hence, the shift observed in Fig. 4 is indeed caused by the change in optics due to the SiN_x layer. This is because the ordinate in Fig. 4 represents *illumination* (or *external generation* as defined by the reference cell calibration) and *not* internal generation of charge carriers in the measured wafer. Thus, the dashed line denotes 1 sun-equivalent illumination of the sample. The optical factor is then used to scale the internal generation in comparison with the reference cell $G_{\rm int} = f \cdot G_{\rm ext}$ taking the optical loss *relative to the reference cell* into account. In our case, the relation of the two optical factors was $f_{\rm SiNx}/f_{\rm blank} \approx 1.39$. So, in first approximation, this would mean that the internal generation is about 39% higher when measuring with the SiN_x-coated side facing the flash lamp, leading consequently to a higher Δn and, thus to the higher $iV_{\rm OC}$ at 1 sun illumination. To support this, the measured reflection is shown in Fig. 5 (left). For

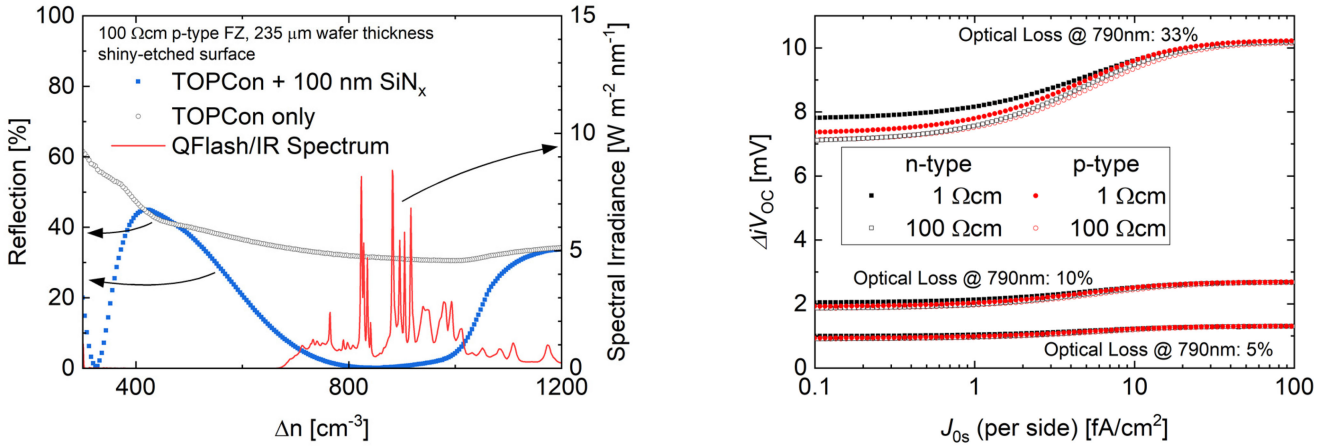

Fig. 5. Left: measurement of the surface reflection for the 100 Ωcm p-type FZ sample measured from both the side that was coated with SiN_x in addition to TOPCon and from the side that was only coated with TOPCon. In addition, the QFlash/IR spectrum is shown [24]. Right: simulated ΔiV_{OC} for 5%, 10%, and 33% in reference to 0% optical loss for monochromatic illumination at 790 nm and a variation of J_{0s}. The simulation was performed for lowly and highly doped n- and p-type material.

the side without SiN_x, the measured reflectance (approximately 30–34 % in the infrared) is similar to that of uncoated c-Si. For the side featuring the additional SiN_x coating, the reflection is below 10% over a broad range in the infrared and a minimum in the reflection is reached at around 850 nm. In addition, the graph shows the QFlash/IR spectrum according to Swirhun [24]. Folding the reflectance curves with the spectrum indicates that the transmission for the SiN_x-coated side will be about 38.4 % higher, which is very close to the quotient of the two optical factors underlining the influence of the reflectance.

Although our data clearly highlight the difference in iV_{OC} for well passivated samples, it is unclear how the change in the internal generation will affect the iV_{OC} at a lower iV_{OC} level. Since with increased recombination (and, thus decreased L_{eff}) it is harder to achieve comparable measurements, the effect was simulated using Quokka3. To simplify things, monochromatic illumination was chosen for this simulation. The results for the QFlash/IR spectrum would be similar. Figure 5 (right) shows the simulated ΔiV_{OC} in dependence on the J_{0s} applied to either side for lowly and highly doped n- and p-type samples.

Here, three levels for the optics are given. The simulations were performed for 5%, 10%, and 33% optical loss, where the first roughly corresponds to a typical, metallized solar cell with textured front surface and the last to a blank, planar silicon surface. For 5% optical loss, the influence is very small and remains at approximately 1.5 mV over the whole range of investigated J_{0s}. For 10% optical loss, the ΔiV_{OC} is higher and slightly increases with increasing J_{0s}, but remains below 3 mV. However, for the higher loss of 33%, the effect is more pronounced with ΔiV_{OC} increasing with increasing J_{0s} from around 7–8 mV up to over 10 mV. This S-shape observed in the graph is caused by the change from Auger (low J_{0s}) to surface recombination (high J_{0s}) as the dominant recombination path.

The discussed influence of the optics on iV_{OC} especially has to be considered in experiments where the iV_{OC} before and after application of an optical layer is to be investigated. Examples for this are: first, comparing the passivation quality of samples before and after coating with transparent conductive oxide to investigate the process damage during the deposition of the layer, and second, comparing samples before and after coating with, e.g., SiN_x acting as a hydrogen source for the hydrogenation of poly-Si layers. It would be possible to eliminate this difference if, instead of a common *external* generation rate, a common *internal* generation rate is defined and, thus correcting for the optical losses while leaving only recombination losses. However, it has to be kept in mind that in this case, the determined value does not relate to the external V_{OC} of solar cells anymore since this always includes optical losses. Therefore, and since such an alternative definition could introduce confusion, its usage should be generally avoided if possible or clearly pointed out otherwise.

D. Influence of Light Trapping and Spectrum

The V_{OC} of solar cells is measured using standardized testing conditions: 1 sun illumination with the AM1.5g spectrum. The typical measurement tools for lifetime measurements, however, often use light sources like a flash lamp, laser, or LED. The spectrum of these light sources can differ strongly from the AM1.5g spectrum. In addition, filters (e.g., the IR filter in the Sinton lifetime tester) may be used to distribute the generation more homogeneously over the sample depth (i.e., wafer thickness), modifying the spectrum, even further. For typical samples structures and wafer thicknesses, this is normally corrected within the calibration of the tools. If, however, diverting away from typical sample properties the calibration can be inaccurate. As a result, the acquired iV_{OC} would be an inaccurate representation of the iV_{OC} for the 1 sun AM1.5g spectrum.

Figure 6 shows the simulated difference between the iV_{OC} corresponding to a selection of different spectra and the iV_{OC} corresponding to the AM1.5g spectrum (hereafter "reference iV_{OC}") in dependence of the wafer thickness. For each spectrum, the graph shows two simulated lines for a sample with planar surfaces: dashed for no rear side reflector (i.e., "worst case")

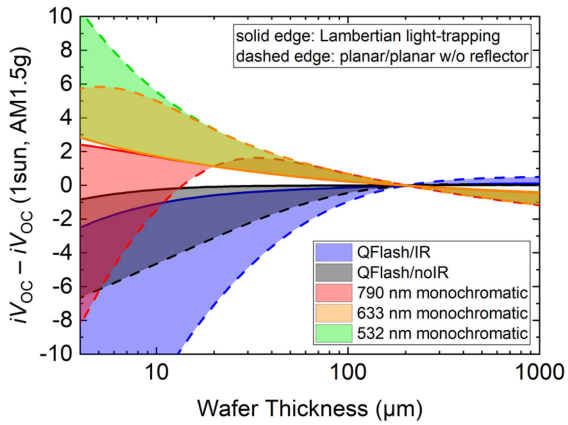

Fig. 6. Simulated difference between the simulated iV_{OC} for 5 spectra (QFlash/IR, Qflash/noIR as well as monochromatic excitation) and the AM1.5g spectrum for 1 sun illumination for a variation of the wafer thickness. Transmission of 100% at the front side was assumed. At the rear side either Lambertian light trapping (solid lines, Green) or a planar/planar structure without any reflector (dashed lines, Macintosh) was assumed. The former should reflect a best-case scenario, whereas the latter should correspond to a worst-case scenario. Most other forms of light trapping parameterizations should fall in between the two, indicated by the area fill between the lines. The illumination intensity with each spectrum was adjusted such that the simulated iV_{OC} at a typical wafer thickness of 200 μm matches that of the corresponding AM1.5g simulation.

and solid for Lambertian (i.e., "best case") light trapping. The front side reflectance was assumed to be negligible. The graph also includes a shaded area between the two lines indicating the range where other cases of light trapping concepts would be expected. Since the iV_{OC} for each spectrum was normalized at a typical wafer thickness of 200 μm, this is where all curves zero out. At lower wafer thicknesses a significant difference to the reference iV_{OC} can be observed, especially for wafer thicknesses less than 100 μm. In the following, the focus will be on this range (wafer thickness $\leq$ 200 μm). The curves can be divided into three categories: first, curves that underestimate iV_{OC} (QSSPC/IR and QFlash/noIR), second, curves that overestimate iV_{OC} (532 nm and 633 nm monochromatic), and last, 790 nm monochromatic, which does either, depending on the wafer thickness and amount of light trapping.

These three categories can be directly related to the amount of infrared light in their spectrum in comparison to the AM1.5g spectrum. For e.g., the QFlash/IR spectrum provides the highest fraction of infrared light and, thus is more sensitive to light trapping and stronger variations are observed. Therefore, when using this spectrum, e.g., at a wafer thickness of 30 μm the iV_{OC} will be underestimated by about 5 mV in the worst-case scenario. Leaving the IR filter out will decrease the difference to about 2 mV at 30 μm thickness, as for this spectrum the IR light contributes less to the minority charge carrier generation. However, despite the lower amount of IR light, both the dashed and solid lines for both of these spectra remain below zero for lower wafer thicknesses, which means that, even without the IR filter light trapping plays a bigger effect for the QFlash spectrum than for the AM1.5g spectrum.

The influence of the excitation wavelengths can be nicely seen for monochromatic excitation. The lowest wavelength of 532 nm leads to the strongest over estimation, since for this wavelength, even at very low thicknesses, the influence of light trapping is negligible. Increasing the wavelength to 633 nm gives the same curve for Lambertian light trapping, but for bad light trapping, a peak at around 5 μm can now be observed due to the influence of light trapping setting in at a thickness of around 15 μm. For both of these curves, it might at first be confusing why the worst-case scenario should lead to a stronger overestimation of the iV_{OC} than the Lambertian case, given that the latter would be expected to yield a higher generation and, thus a higher iV_{OC} at the same illumination intensity. While this is true, the same is the case for the reference iV_{OC} as well and due to the infrared portion present in the AM1.5g spectrum the calculated difference between the iV_{OC} and the reference iV_{OC} is larger for the case of bad light trapping. This also explains the more complicated shape of the red area corresponding to 790 nm excitation where a cross-over point between the solid and dashed lines at around 20 μm can be observed. The red dashed line follows the green and orange dashed lines until a wafer thickness of around 60 μm. This is the thickness where light trapping at this wavelength starts to be significant resulting in a strong dependence of the generation – and, thus the iV_{OC} – on the wafer thickness.

In general, these effects are similar to the spectrum-related corrections done for sun simulators and can be (and should be) corrected if measuring samples with lower thickness. However, this means that in such a case, the spectrum of the light source and the optical properties of the sample have to be well known.

E. Combination of Influences

In the introduction, the iV_{OC} values for two types of samples was given, raising the question whether the two samples can be compared regarding the surface passivation quality: first, FZ 1 Ωcm *n*-type with 200 μm thickness yielding an iV_{OC} of 737 mV, and second, solar-grade Cz 5 Ωcm *n*-type sample with 150 μm thickness yielding an iV_{OC} of 754 mV. From the effects discussed previously, it should be clear that this is not the case. Instead, the difference is mainly due to the change in the sample properties, like the lower thickness and base doping as well as the higher internal generation due to the optical SiN_x layer on the Cz wafer. For further analysis, device simulations were performed changing the respective properties stepwise.

The results for both the experimental data and the corresponding simulation are visualized in Fig. 7. The graph gives not only the data for the respective samples, but also the single steps if certain aspects in the sample parameters are changed. Two routes are described in the graph, the lower route where the change in J_{0s} is applied first and the upper route where it is applied last. Since the determined J_{0s} for the Cz sample (0.5 fA/cm^2) is higher than for the FZ sample (0.2 fA/cm^2), the change in J_{0s} results in a slight reduction of iV_{OC} of –1.2 mV if applied first and –1.4 mV if applied last. As shown in the graph, the increase in iV_{OC} mainly originates from the other changes in the sample properties, namely the base resistivity (ρ_b), the wafer thickness (w), and the surface reflectance (R), where each contribute roughly one third to the total increase.

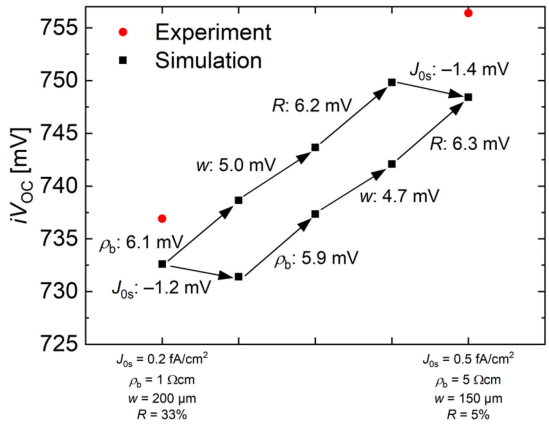

Fig. 7. Measured and simulated iV_{OC} with the single influences surface passivation (J_{0s}), base doping (ρ_b), wafer thickness (w) and reflectance (R) changed step by step with the J_{0s} change being applied first (lower route) or last (upper route). The numbers next to each symbol give the increase or decrease in $\boldsymbol{iV}_{OC}$ due to changing this parameter. The corresponding parameters for the two samples are given as a label on the abscissa.

Although there is a certain discrepancy between the measured and the simulated iV_{OC} (again, at least partly due to the Auger parameterization), the general trend of the simulated steps – especially relative to the other influences – should be representative for the two samples. This indicates that in our case, less than 10% of the change in iV_{OC} stems from a change in the surface passivation quality and the total change in iV_{OC} is positive and not negative as the change in J_{0s} would indicate. Therefore, it is clear that in this case, the values for iV_{OC} cannot be used to judge the surface passivation quality.

VI. Alternatives

For the purpose of describing the surface passivation quality, the usage of J_{0s} (or J_{0e} in case of diffused surfaces) is an appropriate alternative [25], [26]. In contrast with iV_{OC}, J_{0s} does not depend on the base doping for typical boundary conditions (e.g., SiN_x or Al_2O_3 passivation) and is independent from the wafer thickness, bulk recombination, and optics, thus only describing surface recombination [5]. Instead, the only strong influence is the temperature. e.g., the change from 25°C (298.15 K) to 300 K results in an increase in J_{0s} by 30–40% due to the strong dependence of $n_{i,eff}^2$ on the temperature. Although the temperature is standardized for the measurements with the lifetime tester, it still should be noted when presenting J_{0s} values. The main problem with J_{0s} however is – as was the case earlier – that the evaluated J_{0s} is strongly tightened to the used parameterization for the bulk recombination. Hence, the quality of the evaluated J_{0s} depends on the quality of this parameterization and the modeling of the lifetime data [6]–[9]. As we have reached a point where many research groups reported lifetimes exceeding the level predicted by the typically used Richter Auger model, there is a limitation in the usage of J_{0s} as a way to characterize surface recombination, especially on n-type Si samples. Thus, once a new Auger parameterization is available, all J_{0s} values need to be re-evaluated and corrected corresponding to the new parameterization, if desiring a comparable value to describe the surface recombination. Unfortunately, this is an inherent problem with the concept of trying to separate the different contributions to the total recombination rate. This problem can be worked around to some degree if thinner, lowly doped wafers are chosen, since this increases the relative contribution of J_{0s} to the total J_0 of the wafer and, thus the J_{0s} evaluation is more reliable. However, the wafer thickness should not be chosen too thin to avoid complications as outlined in Section V-D. Thus, a thickness of 120–150 μm is a good compromise. Another way to solve this is by varying the thickness of the wafers within an experiment and then fitting the base and surface recombination rates for each Δn as e.g., demonstrated by Yablonovitch *et al.* [27]. This way the bulk recombination rate does not have to be known upfront and can be determined during the experiment. However, this approach should be carried out carefully, since it must be ensured that the passivation technology performs equally on all wafer thicknesses. A second problem that can occur is photon recycling as mentioned in Section V-B. Since the radiative and surface recombination rates both are proportional to the $n \cdot p$ product, a thickness-dependent contribution of the radiative recombination (as would be the case with photon recycling) is indistinguishable from surface recombination and can result in an additional systematic uncertainty in J_{0s}, if not corrected. As mentioned in Section V-B, if evaluating at higher Δn close to 1 sun illumination, the influence of the radiative recombination is low and photon recycling should not be problematic. However, at lower Δn, this effect has to be considered. In all cases, the evaluation of J_{0s} works best if the contribution of J_{0s} to the total J_0 is large, either by reducing other recombination rates (via thickness or doping) or if J_{0s} itself is at least as high as the J_0 contribution of the bulk (which, for high-quality Si material, is usually in the range of 5–10 fA/cm^2 depending on the wafer thickness and doping).

Another parameter that is often used to describe the surface recombination is the effective surface recombination velocity S_{eff}. However, it is only independent from the base doping concentration if band bending is negligible [5]. In addition, it is typically injection dependent for medium to high Δn. Therefore – just like published lifetime values – it should only be given together with the base doping concentration and the minority charge carrier density at which it was determined. For more details on the usage of J_{0s} and S_{eff}, please refer to the very comprehensive papers by McIntosh and Black [5] as well as Cuevas and MacDonald [26]. One advantage of S_{eff} over J_{0s} (or rather J_{0b} in this case) in the case of solar cells is, that it may even be determined by measuring the spectral response of a solar cell [28]. However, if S_{eff} is low (i.e., the surface passivation is good), the uncertainty of S_{eff} will be high, which means that this method is mainly useful for cells with relatively low V_{OC} and η. In general, an evaluation of J_{0s}, if possible, should be preferred over S_{eff}.

A completely different approach to parameterizing the surface recombination, for the case of passivated surfaces without significant surface doping, is to specify the interface trap density D_{it} and the fixed charge carrier density Q_f at the interface. These

parameters can be determined e.g., from capacitance-voltage [29], surface photovoltage [30], or COCOS [31] measurements. D_{it} and Q_{f} in turn can then be used to model the surface recombination and hence, the lifetime curve. The advantage of using these parameters is that they can be measured independently from (and then compared with) the measurement of the minority charge carrier lifetime. However, modeling the lifetime based on D_{it} and Q_{f} does again require detailed parameterization of the bulk recombination. An additional problem with these methods is that they are prone to measurement errors due to leakage currents and, thus cannot be (easily) used for every type of surface passivation coating, especially if the coating is conductive.

In those cases where none of the mentioned alternatives can be evaluated, iV_{OC} can be an option to quantify the differences in surface passivation quality within a *comparable* set (similar optics, thickness, and base doping) of samples. However, it should be kept in mind that especially for excellent surface passivation the sensitivity to the change in surface passivation is low and often masked by measurement uncertainties.

It is worth mentioning that the mentioned alternatives only describe a certain model for the surface recombination. In general, surface recombination may exhibit a more complex injection dependence meaning that it is not possible to model the curve using $J_{0\mathrm{s}}$, S_{eff} or D_{it}, and Q_{f}, or possibly only for some part of the curve. Here, iV_{OC} has the advantage that it can always be evaluated as long as 1 sun illumination is reached during the measurement. However, it should be kept in mind that in such a case iV_{OC} only reveals a small part of the picture, since it only describes the recombination at a single Δn and does not reflect the injection dependence of the recombination.

As a final remark, although we advise against using iV_{OC} to describe the surface recombination, it can be very useful, if not the surface recombination *specifically* is of interest, but the *total* recombination. This is, e.g., the case for the characterization of solar cell precursors to judge their performance at different stages of processing. In this case, iV_{OC} can be related directly to V_{OC}, if the optical properties of the precursor are similar to that of the final cell (i.e., "blue" precursor).

VII. Conclusion

In this article, the influence of the base doping, surface passivation quality, wafer thickness, and sample optics on the determined iV_{OC} was discussed in detail. Due to these influences, one needs to be careful when using iV_{OC} as a direct measure for the surface passivation quality since the comparability of the samples needs to be ensured and such comparability across several experiments is usually quite limited. This is especially the case for excellent surface passivation where its influence on iV_{OC} becomes negligible. An example of two sample types (denoted FZ and Cz), as used typically in the photovoltaic research community, was given demonstrating the combination of all of these influences resulting in an iV_{OC} of 737 mV for the FZ sample and 754 mV for the Cz sample despite the former featuring the better surface passivation. As an alternative, we recommend the use of $J_{0\mathrm{s}}$, since it is independent of most sample parameters for common passivation technologies. In those cases, where a $J_{0\mathrm{s}}$ cannot be determined confidently, the iV_{OC} might still be a very useful parameter as long as the mentioned influences in the experiments are negligible or clearly stated besides the iV_{OC}. It should, however, be kept in mind that comparisons across multiple sample sets with varying optics, thickness, and base doping cannot be easily performed. This is especially the case for comparisons of iV_{OC} data from different publications as in many cases these sample parameters are not well known, if known at all. Nevertheless, there are cases where iV_{OC} is of particular usefulness if the differences in *total* recombination are of interest. An example for such a case is the characterization of solar cell precursors at different stages of processing to predict the V_{OC} of finished cells made from *these specific* precursors.

Acknowledgment

The authors would like to thank P. Barth, F. Feldmann, N. Jung, L. Kraus, A. Leimenstoll, J.-I. Polzin, F. Schätzle, and L. Schönleber for processing of the samples and Felix Martin for the reflectance measurements.

References

[1] A. Onno, C. Chen, P. Koswatta, M. Boccard, and Z. C. Holman, "Passivation, conductivity, and selectivity in solar cell contacts: Concepts and simulations based on a unified partial-resistances framework," *J. Appl. Phys.*, vol. 126, no. 18, 2019, Art. no. 183103.

[2] W. Shockley, "The theory of p-n junctions in semiconductors and p-n junction transistors," *Bell System Tech. J.*, vol. 28, no. 3, pp. 435–489, 1949.

[3] A. Cuevas and R. A. Sinton, "Prediction of the open-circuit voltage of solar cells from the steady-state photoconductance," *Prog. Photovolt: Res. Appl.*, vol. 5, pp. 79–90, 1997.

[4] J. A. Giesecke, M. C. Schubert, B. Michl, F. Schindler, and W. Warta, "Minority carrier lifetime imaging of silicon wafers calibrated by quasi-steady-state photoluminescence," *Sol. Energy Mater. Sol. Cells*, vol. 95, no. 3, pp. 1011–1018, 2011.

[5] K. R. McIntosh and L. E. Black, "On effective surface recombination parameters," *J. Appl. Phys.*, vol. 116, no. 1, 2014, Art. no. 14503.

[6] A. Kimmerle, J. Greulich, and A. Wolf, "Carrier-diffusion corrected J0-analysis of charge carrier lifetime measurements for increased consistency," *Sol. Energy Mater. Sol. Cells*, vol. 142, pp. 116–122, 2015.

[7] H. Mäckel and K. Varner, "On the determination of the emitter saturation current density from lifetime measurements of silicon devices," *Prog. Photovolt: Res. Appl.*, vol. 21, pp. 850–866, 2012, doi: 10.1002/pip.2167.

[8] D. E. Kane and R. M. Swanson, "Measurement of the emitter saturation current by a contactless photoconductivity decay method (silicon solar cells)," in *Proc. 18th IEEE Photovoltaic Specialists Conf.*, 1985, pp. 578–583.

[9] C. Reichel, F. Granek, J. Benick, O. Schultz-Wittmann, and S. W. Glunz, "Comparison of emitter saturation current densities determined by quasi-steady-state photoconductance measurements of effective carrier lifetimes at high and low injections," in *Proc. 23rd Eur. Photovolt. Sol. Energy Conf. Exhibit.*, 2008, pp. 1664–1669.

[10] T. Niewelt *et al.*, "Taking monocrystalline silicon to the ultimate lifetime limit," *EuroSun2004*, vol. 185, pp. 252–259, 2018.

[11] H. Nagel, C. Berge, and A. G. Aberle, "Generalized analysis of quasi-steady-state and quasi-transient measurements of carrier lifetimes in semiconductors," *J. Appl. Phys.*, vol. 86, no. 11, pp. 6218–6221, 1999.

[12] A. Richter, S. W. Glunz, F. Werner, J. Schmidt, and A. Cuevas, "Improved quantitative description of auger recombination in crystalline silicon," *Phys. Rev. B*, vol. 86, no. 16, , 2012, Art. no. 165202.

[13] P. P. Altermatt *et al.*, "Injection dependence of spontaneous radiative recombination in crystalline silicon: Experimental verification and theoretical analysis," *Appl. Phys. Lett.*, vol. 88, no. 26, 2006, Art. no. 261901.

[14] A. Fell, J. Schön, M. C. Schubert, and S. W. Glunz, "The concept of skins for silicon solar cell modeling," *Sol. Energy Mater. Sol. Cells*, vol. 173, pp. 128–133, 2017.

[15] M. A. Green, "Lambertian light trapping in textured solar cells and light-emitting diodes: Analytical solutions," *Prog. Photovolt: Res. Appl.*, vol. 10, no. 4, pp. 235–241, 2002.
[16] K. R. McIntosh and S. C. Baker-Finch, "A parameterization of light trapping in wafer-based solar cells," *IEEE J. Photovolt.*, vol. 5, no. 6, pp. 1563–1570, Nov. 2015.
[17] B. A. Veith-Wolf and J. Schmidt, "Unexpectedly high minority-carrier lifetimes exceeding 20 ms measured on 1.4-Ω cm n -Type silicon wafers," *Phys. Status Solidi RRL*, vol. 90, 2017, Art. no. 1700235.
[18] B. A. Veith-Wolf, S. Schäfer, R. Brendel, and J. Schmidt, "Reassessment of intrinsic lifetime limit in n-type crystalline silicon and implication on maximum solar cell efficiency," *Sol. Energy Mater. Sol. Cells*, vol. 186, pp. 194–199, 2018.
[19] L. E. Black and D. H. Macdonald, "Accounting for the dependence of coil sensitivity on sample thickness and lift-off in inductively coupled photoconductance measurements," *IEEE J. Photovolt.*, vol. 9, no. 6, pp. 1563–1574, Nov. 2019.
[20] S. Y. Herasimenka, W. J. Dauksher, and S. G. Bowden, "$>$750 mV open circuit voltage measured on 50 μm thick silicon heterojunction solar cell," *Appl. Phys. Lett.*, vol. 103, no. 5, 2013, Art. no. 53511.
[21] A. Augusto, E. Looney, C. del Cañizo, S. G. Bowden, and T. Buonassisi, "Thin silicon solar cells: Pathway to cost-effective and defect-tolerant cell design," *Energy Procedia*, vol. 124, pp. 706–711, 2017.
[22] A. Augusto, P. Balaji, J. Karas, and S. G. Bowden, "Impact of substrate thickness on the surface passivation in high performance n-type solar cells," in *Proc. 7th World Conf. Photovoltaic Energy Convers.*, Waikoloa, HI, 2018, pp. 2792–2794.
[23] M. A. Green, "Limits on the open-circuit voltage and efficiency of silicon solar cells imposed by intrinsic auger processes," *IEEE Trans. Electron Devices*, vol. 31, no. 5, pp. 671–678, May 1984.
[24] J. S. Swirhun, R. A. Sinton, M. K. Forsyth, and T. Mankad, "Contactless measurement of minority carrier lifetime in silicon ingots and bricks," *Prog. Photovolt: Res. Appl.*, vol. 19, no. 3, pp. 313–319, 2011.
[25] A. Cuevas, "The recombination parameter J0," *Energy Procedia*, vol. 55, pp. 53–62, 2014.
[26] A. Cuevas and D. Macdonald, "Measuring and interpreting the lifetime of silicon wafers," *Sol. Energy*, vol. 76, no. 1-3, pp. 255–262, 2004.
[27] E. Yablonovitch, D. Allara, C. Chang, T. Gmitter, and T. Bright, "Unusually low surface-recombination velocity on silicon and germanium surfaces," *Phys. Rev. Lett.*, vol. 57, no. 2, pp. 249–252, 1986.
[28] P. A. Basore, "Extended spectral analysis of internal quantum efficiency," in *Proc. 23rd IEEE Photovolt. Specialists Conf. Louisville*, 1993, pp. 147–152.
[29] R. B. M. Girisch, R. P. Mertens, and R. F. de Keersmaecker, "Determination of $SiSiO_2$ interface recombination parameters using a gate-controlled point-junction diode under illumination," *IEEE Trans. Electron Devices*, vol. 35, no. 2, pp. 203–222, Feb. 1988.
[30] D. K. Schroder, "Surface voltage and surface photovoltage: History, theory and applications," *Meas. Sci. Technol.*, vol. 12, no. 3, pp. R16–R31, 2001.
[31] M. Wilson, J. Lagowski, A. Savtchouk, L. Jastrzebski, and J. D'Amico, "COCOS (Corona oxide characterization of semiconductor) metrology: Physical principles and applications," in *Gate Dielectric Integrity: Material, Process, and Tool Qualification*, D. C. Gupta and G. A. Brown, Eds., West Conshohocken, PA, USA: ASTM Int., 2000, pp. 74–74–17.